Observer-based Event-triggered Model-free Adaptive Sliding Mode Predictive Control

Bing Ren[1,2] and Guangqing Bao[3*]

[1] College of Electrical and Information Engineering, Lanzhou University of Technology, Lanzhou, China
[2] School of Automation and Electrical Engineering, Lanzhou Jiaotong University, Lanzhou, China
[3] School of Electronics & Information Engineering, Southwest Petroleum University, Chengdu, China
[*] Corresponding author. E-mail: baogq03@163.com

Received: Apr. 10, 2022; Accepted: Jul. 26, 2023

For simple-input and simple-output (SISO) discrete-time nonlinear systems, an observer-based event-triggered model-free adaptive sliding mode predictive control technique (EMFASPC) is put forth in this study. The estimate of pseudo partial derivatives (PPD) and the transmission of I/O data are both carried out aperiodically at the time of event triggering to conserve network resources. A unified framework of event-triggered model-free adaptive control with an adaptive observer and an event-triggered PPD estimation method is constructed based on the equivalent data model after compact format dynamic linearization (CFDL). The controller part adopts integral sliding mode control (SMC) combined with a rolling optimization idea of model predictive control (MPC) to predict the expected trajectory of the sliding mode state and generate the optimal control input. According to the relationship among the system tracking error, current measurement data, and the previous trigger time output, the event trigger condition is set to determine the next event trigger time, which reduces the unnecessary transmission on the premise of system stability. The stability performance of the closed-loop system is analyzed by the Lyapunov method. Finally, numerical simulation and the shell-and-tube heat exchanger control system simulation are carried out to verify that the proposed algorithm has good robustness and tracking accuracy under the limited bandwidth and computing resources

Keywords: Adaptive observer, Compact format dynamic linearization, Event-triggered, Sliding mode predictive control, Model-free adaptive control

http://dx.doi.org/10.6180/jase.202405_27(5).0010

1. Introduction

With the development of information technology, the use of data-driven techniques to process massive amounts of online data carrying dynamic information has become a hot topic of research in the current control theory community. Among many data-driven control methods, model-free adaptive control (MFAC) with unique dynamic linearization (DL) method (equivalent DL data model replaces the traditional approximately linearization model), novel PPD (virtual parameters), and excellent adaptive capability [1], has received much attention and achieved notable achievements. For example, [2] and [3] implemented the bounded-input bounded-output stability and tracking error monotonic convergence analysis for partial-format and full-format DL techniques, respectively. [4] proposed a new observer-based MFAC method and extend the study [5]. [6] adds terminal sliding mode control to the traditional MFAC system to improve the anti-disturbance capability. In addition, there are also studies in motion control systems [7], industrial control systems [8], energy control systems [9], and other applications.

The traditional MFAC method does not consider the

variation between data but instead simply transmits data at a fixed period, resulting in a double waste of network and computational resources. The data of two adjacent sampling intervals are likely unchanged or not very different and do not affect the steady state of dynamic performance. As with adding a judgment box holding a trigger mechanisms to the control flowchart, event-triggered control is driven by monitoring events rather than the passage of time. If the trigger mechanism fulfills the trigger conditions for sequential execution, the data can go to the next actuator. In recent years, research on transmission-based event-triggered control has made great progress, from linear systems [10] to nonlinear systems [11], from continuous systems [12] to discrete systems [13], from centralized systems [14] to distributed systems [15] and multi-intelligent body systems [16] and so on. Among them, [12] develops two types of controllers for model-based singularly perturbed nonlinear systems with slow dynamics, ensuring different asymptotic stability properties; [13] uses event-driven neural dynamic programming to design approximate optimal control strategies, with the appropriate number of events to ensure the required approximate accuracy; [15] presents the optimization problem of maximizing the trigger threshold with a sensor network communication mechanism, achieving satisfactory filtering performance. Unfortunately, the aforementioned event-triggered controllers are model-based designs, which makes it challenging for them to be applied to many real-world systems.

To solve the bandwidth-constrained problem of unknown nonlinear systems that are difficult to build accurate mathematical models, it is a good choice to combine event-triggered control ideas and MFAC theory. At present, some scholars have carried out related research. [17] replaces a single input increment with a set of input-output data increments in the DL method, and chooses a radial basis function neural network to approximate the PPD, which only causes event triggering when the input-output data changes sufficiently, saving the cost of transmission, but the introduced radial basis function increases the burden of computation. [18] introduces a non-periodic neural network weight update law method in the parameter estimation of the controller to achieve an on-demand update of the controller. [19] proposes an event-triggered MFAC scheme based on offline parameter identification under three different DL methods, and sets the triggering conditions based on Liapunov functions. [20] adds a prediction compensation module to the control framework, and the results show that the event-triggered multi-step prediction compensation algorithm can effectively prevent data loss from jamming attacks or continuous attacks. [21] investigates the model-free adaptive event-triggered tracking control problem with unknown bounded disturbances, designs unknown disturbance estimators, and incorporates disturbance compensation in the controller to make the tracking error converge. Considering the computational pressure and time cost, [22] sets a static threshold event triggering mechanism. [23] investigates the MFAC of an event triggering information-physical fusion system in the case of disinformation injection attacks, and establishes a novel ET-MFAC framework that enables nonlinear systems to overcome attacks and achieve trajectory tracking.

Meanwhile, Sliding mode predictive control combines SMC and MPC [24], which not only can exploit the advantages of SMC in terms of rapidity and robustness but also considers the control optimization problem of entering the sliding mode surface and has received a lot of attention[25–29]. For example, [25] uses the sliding mode predictive controller in a solar air conditioning unit to improve the ability to handle set point variations and suppress disturbances. The sliding mode predictive controller designed by [26] and [27] in the precision motion control system eliminates the system jitter. [28] compensates and solves the time delay and data packet loss problems in the network control system through the sliding mode predictive control idea. To improve the load-tracking capability and robustness of the boiler-turbine unit, [29] designed a discrete-time sliding-mode predictive controller with a dual-mode control law to demonstrate the input state stability of the closed-loop system.

Inspired by the above analysis, this paper designs an observer-based event-triggered model-free adaptive sliding mode predictive control method for discrete-time nonlinear systems to improve the robustness and tracking accuracy of the system under the bandwidth and computational resource constraints. Specifically, the unknown nonlinear system is first converted into an equivalent linear data model based on the CFDL technique, and then an adaptive observer is designed to build an observer-based event-triggered PPD estimation algorithm and model-free adaptive sliding mode predictive controller based on the idea of the transmission-based event triggering. The PPD and control input updates are no longer triggered by a fixed period, but by satisfying the designed event triggers generated after satisfying the designed event triggering mechanism. The combination of a sliding mode control and MPC improves the control accuracy and robustness by considering the optimal control input for each trigger moment. The main contributions of this paper include: 1) compared with the traditional MFAC, the proposed method updates the PPD and control inputs acyclically, reducing the utilization

of computational resources and unnecessary data transmission; 2) compared with the traditional event-triggered control, the proposed method is based on a data-driven approach that does not rely on the structure and parameter information of the mathematical model, avoiding the model deviation or inaccurate 3) the combination of sliding mode control and predictive control ensures fast convergence speed while optimizing the motion trajectory.

The remainder of the paper is divided into the following sections. An equivalent data model is created in Section II. Section III provides specifics on the EMFASPC scheme's design process and related stability analysis. Results of numerical simulation and simulation of a shell and tube heat exchanger system are presented in Section IV. This paper is summarized in Section V.

2. Problem statement

2.1. Equivalent data model

Consider the SISO discrete-time nonlinear system as follows:

$$\begin{aligned} y(k+1) = f(&y(k), y(k-1), \\ &\cdots, y\left(k-l_y\right), u(k), u(k-1), \cdots, u\left(k-l_u\right)) \end{aligned} \tag{1}$$

where $y(k)$ and $u(k)$ are the system output and input, $f(\cdot)$ is the unknown nonlinear function, and l_y and l_u are the unknown orders of the $y(k)$ and $u(k)$, respectively. The following assumptions need to be made before DL:

Assumption 1. The partial derivative of f$(\cdot)$ with respect to control input u(k) is continuous.

Assumption 2. The system Eq. (1) is generalized Lipschitz, that is, $|\Delta y(k+1)| \leq c_\varphi |\Delta u(k)|$ for any k and $\Delta u(k) \neq 0$, where $\Delta y(k+1) = y(k+1) - y(k)$ is output data increment, $\Delta u(k) = u(k) - u(k-1)$ is input data increment and c_φ is a positive constant.

Assumption 1 is a prerequisite for the controllability of the system, and assumption 2 is a manifestation of the law of energy conservation in the control system, so the assumption is reasonable. Based on this, the system Eq. (1) can be expressed in the form of a CFDL data model as:

$$\Delta y(k+1) = \varphi(k)\Delta u(k) \tag{2}$$

where $\varphi(k)$ is PPD and represents the virtual input incremental gain at the moment k.

Remark 1. $\varphi(k)$ is a fictitious parameter rather than an actual parameter that exists. All potentially complex behaviors of the original dynamic nonlinear system, including nonlinearity, time-varying parameters or structure, are condensed and merged into this parameter. However, the numerical behavior of $\varphi(k)$ is relatively simple and can be estimated by choosing a suitable adaptive algorithm that satisfies $|\varphi(k)| \leq c_\varphi$

2.2. Observer-based event-driven PPD estimation algorithm

$\varphi(k)$ is estimated using an adaptive observer, and the observer structure is first established:

$$\hat{y}_a(k+1) = \hat{y}_a(k) + \hat{\varphi}(k)\Delta u(k) + K_a \varepsilon_a(k) \tag{3}$$

where $\hat{y}_a(k)$ denote the output estimates, and $\hat{\varphi}(k)$ denotes the estimate of the PPD. K_a is the observation error gain satisfying $0 < K_a < 1$. Let $\varepsilon_a(k)$ denote the output estimation error, and the following relation is available:

$$\varepsilon_a(k) = y(k) - \hat{y}_a(k) \tag{4}$$

Substituting Eqs. (2) and (3), one can obtain:

$$\varepsilon_a(k+1) = (1 - K_a)\,\varepsilon_a(k) + \breve{\varphi}(k)\Delta u(k) \tag{5}$$

Where $\breve{\varphi}(k) = \varphi(k) - \hat{\varphi}(k)$, denotes the PPD estimation error.

In addition, considering $e_a(k+1)$ is not directly available, with the help of the two-step delayed uncertain parameter estimation technique of $e_s(k+1) \approx 2\varepsilon_a(k) - \varepsilon_a(k-1)$ to be estimated, a new descriptive form of $y(k+1)$ is made from the meaning of the output estimation error:

$$\begin{aligned} &y(k+1) = \hat{y}_a(k) + \\ &\Delta u(k)\hat{\varphi}(k) - \varepsilon_a(k-1) + (2 + K_a)\,\varepsilon_a(k) \end{aligned} \tag{6}$$

The observer-based algorithm for estimating the PPD is as follows:

$$\hat{\varphi}(k+1) = \hat{\varphi}(k) + 2\Delta u(k)\left(|\Delta u(k)|^2 + \sigma\right)^{-1} E(k) \tag{7}$$

Where σ denotes the penalty factor, $\sigma > 0$, and $E(k) = \varepsilon_a(k+1) - (1 - K_a)\,\varepsilon_a(k)$.

Remark 2. The above estimation algorithm is time-triggered, i.e., the PPD estimates are updated with a fixed sampling period, which greatly wastes computational resources and network bandwidth. By introducing an event-triggered factor in the estimation algorithm, it is updated only when an event occurs.

The addition of the event-triggered operator and the joint reset algorithm constitute the new PPD estimation algorithm:

$$\begin{aligned} &\hat{\varphi}(k+1) = \hat{\varphi}(k) + \beta(k)\frac{2\Delta u(k)E(k)}{|\Delta u(k)|^2 + \sigma} \\ &\hat{\varphi}(k) = \hat{\varphi}(1) \quad |\hat{\varphi}(k)| \leq \delta \\ &\text{or } |\Delta u(k)| \leq \delta \end{aligned} \tag{8}$$

Where δ is a sufficiently small positive number to guarantee the tracking performance of the PPD. $\beta(k)$ represents the index operator, with $\beta(k) = 1$ at the trigger moment and $\beta(k) = 0$ at the non-trigger instant.

The control objective of this paper is to design an observer-based event-triggered PPD estimation algorithm and EMFASPC scheme based on the data model to drive a discrete-time nonlinear system of unknown structure to track the desired trajectory.

3. Data-driven controller design and stability analysis

This section proposes an observer-based and event-triggered EMFASPC scheme. The addition of the transmission-based event-triggering idea modifies the original fixed-cycle triggering mechanism, and stability analysis is carried out using the Lyapunov theory.

3.1. Sliding mode predictive control

Define the integral sliding mode surface function as follows:

$$\lambda(k) = \varepsilon(k) + m\sum_{h=1}^{k} T\varepsilon(h) \tag{9}$$

where m is the coefficient of the integral term satisfying $m > 0, T$ denotes the sampling interval, and $\varepsilon(k)$ denotes the systematic tracking error, i.e. $\varepsilon(k) = y_d(k) - y(k)$, where the given output satisfies $|y_d(k)| \le A$

Consider the sliding mode surface satisfies the relation $\Delta\lambda(k+1) = \lambda(k+1) - \lambda(k) = 0$, and the equivalent control $u_1(k)$ is obtained by Eq. (9):

$$\begin{aligned} u_1(k) = &\frac{\hat{\varphi}(k)}{\hat{\varphi}^2(k)+\tau} \\ &(y_d(k+1) - \hat{y}_a(k) - \\ &(2+K_a)\,\varepsilon_a(k) + \varepsilon_a(k-1) - \frac{\varepsilon(k)}{1+mT}\Big) \end{aligned} \tag{10}$$

Where $\tau > 0$.

Remark 3. SMC typically consists of two stages: the sliding surface stage and the sliding stage entering the sliding surface. The sliding surface stage is subjected to equivalent control. MPC is chosen in this paper during the sliding surface entry process to maximize the sliding surface function's ideal trajectory.

The predictive control input is defined as $u_2(k)$, combined with Eqs. (6), (9) and (10), the sliding mode surface can be obtained:

$$\begin{aligned} \lambda(k+1) = &\lambda(k) - (1+mT)\hat{\varphi}(k)u_2(k) - \\ &\frac{\tau mT}{\hat{\varphi}^2(k)+\tau}\hat{y}_a(k) + \frac{\tau(1+mT)}{\hat{\varphi}^2(k)+\tau}p(k) \end{aligned} \tag{11}$$

Where $p(k) = y_d(k+1) - \frac{y_d(k)}{1+mT} - \left(2 + K_a - \frac{1}{1+mT}\right)\varepsilon_a(k) + \varepsilon_a(k-1)$.

Define predictive control functions:

$$\begin{aligned} \lambda^a(k) = &\Theta\lambda(k) - \Xi U^a(k-1) - \\ &\Omega Y(k-1) + \Psi P(k-1) \end{aligned} \tag{12}$$

where $\lambda^a(k), U^a(k-1), Y(k-1)$ and $P(k-1)$ can be expressed in the prediction domain as:

$$\lambda^a(k) = \begin{bmatrix} \lambda(k+1) & \lambda(k+2) & \cdots & \lambda(k+N) \end{bmatrix}^T$$

$$U^a(k-1) = \begin{bmatrix} u_2(k) & u_2(k+1) & \vdots & u_2(k+N-1) \end{bmatrix}^T$$

$$Y(k-1) = \begin{bmatrix} \hat{y}_a(k) & \hat{y}_a(k+1) & \cdots & \hat{y}_a(k+N-1) \end{bmatrix}^T$$

$$P(k-1) = \begin{bmatrix} p(k) & p(k+1) & \cdots & p(k+N-1) \end{bmatrix}^T$$

The symbols $\Theta, \Xi, \Omega, \Psi$ are as follows:

$$\Theta = \begin{bmatrix} 1 & 1 & \ldots & 1 \end{bmatrix}^T$$

$$\Xi = (1+mT)\begin{bmatrix} \hat{\varphi}(k) & 0 & \ldots & 0 \\ \hat{\varphi}(k) & \hat{\varphi}(k+1) & \ldots & 0 \\ \vdots & \vdots & \ddots & \vdots \\ \hat{\varphi}(k) & \hat{\varphi}(k+1) & \ldots & \hat{\varphi}(k+N-1) \end{bmatrix}$$

$$\Omega = \begin{bmatrix} \frac{\tau mT}{\hat{\varphi}^2(k)+\tau} & 0 & \cdots & 0 \\ \frac{\tau mT}{\hat{\varphi}^2(k)+\tau} & \frac{\tau mT}{\hat{\varphi}^2(k+1)+\tau} & \cdots & 0 \\ \vdots & \vdots & \ddots & \vdots \\ \frac{\tau mT}{\hat{\varphi}^2(k)+\tau} & \frac{\tau mT}{\hat{\varphi}^2(k+1)+\tau} & \cdots & \frac{\tau mT}{\hat{\varphi}^2(k+N-1)+\tau} \end{bmatrix}$$

$$\Psi = \begin{bmatrix} \frac{\tau(1+mT)}{\hat{\varphi}^2(k)+\tau} & 0 & \cdots & 0 \\ \frac{\tau(1+mT)}{\hat{\varphi}^2(k)+\tau} & \frac{\tau(1+mT)}{\hat{\varphi}^2(k+1)+\tau} & \cdots & 0 \\ \vdots & \vdots & \ddots & \vdots \\ \frac{\tau(1+mT)}{\hat{\varphi}^2(k)+\tau} & \frac{\tau(1+mT)}{\hat{\varphi}^2(k+1)+\tau} & \cdots & \frac{\tau(1+mT)}{\hat{\varphi}^2(k+N-1)+\tau} \end{bmatrix}$$

Assuming that the predictive and control domains are the same, define a cost function:

$$F = \lambda^a(k)^T\lambda^a(k) + vU^a(k-1)^TU^a(k-1) \tag{13}$$

where v is a weight factor used to constrain the predictive control input.

According to the optimal control theory $\frac{\partial F}{\partial U^a(k-1)} = 0$, substitute Eqs. (12) and (13), then the optimal control solution in the prediction range is

$$\begin{aligned} U^a(k) = &-\left((-\Xi)^T(-\Xi) + vI\right)^{-1}(-\Xi)^T \times \\ &(\Theta\lambda(k) - \Omega Y(k-1) + \Psi P(k-1)) \end{aligned} \tag{14}$$

where $\mathrm{Y(k-1)}$ and $\mathrm{P(k-1)}$ contain values for future moments, which are not directly available and the estimated values need to be adopted: $\hat{Y}(k-1) = \begin{bmatrix} \hat{y}_a(k) & \hat{y}_a(k) & \cdots & \hat{y}_a(k) \end{bmatrix}^T$, $\hat{P}(k-1) = \begin{bmatrix} p(k) & p(k) & \cdots & p(k) \end{bmatrix}^T$

The first part of the optimal control is selected as the predictive control function at k time:

$$u_2(k) = -\gamma\left((-\Xi)^T(-\Xi) + vI\right)^{-1}(-\Xi)^T \times (\Theta\lambda(k) - \Omega\hat{Y}(k-1) + \Psi\hat{P}(k-1)) \tag{15}$$

where $\gamma = \begin{bmatrix} 1 & 0 & \cdots & 0 \end{bmatrix}$. Thus, the total control input is formed:

$$\begin{aligned} u(k) &= u(k-1) + u_1(k) + u_2(k) \\ &= \frac{\hat{\varphi}(k)}{\hat{\varphi}^2(k) + \tau}\left(y_d(k+1) - \hat{y}_a(k) - (2 + K_a)\,\varepsilon_a(k) + \varepsilon_a(k-1) - \frac{\varepsilon(k)}{1+mT}\right) + \gamma\left((-\Xi)^T(-\Xi) + vI\right)^{-1}\Xi^T(\Theta\lambda(k) - \Omega\hat{Y}(k-1) + \Psi\hat{P}(k-1)) \end{aligned} \tag{16}$$

3.2. Event-triggered model-free adaptive sliding mode predictive control

Suppose the event trigger instant is k_i , where i=0,1,2, $\cdots$, set the event trigger function:

$$\varrho(k) = |o(k)| - \vartheta|\varepsilon(k)| \tag{17}$$

where $\vartheta > 0$ denotes the event trigger threshold, $o(k) = y(k) - y(k_i)$ denotes the trigger error, and $y(k_i)$ is the output of the most recent event trigger instant.

Set event trigger conditions:

$$k_{i+1} = \inf\{k \in N \mid k > k_i, \varrho(k) > 0\} \tag{18}$$

The trigger condition is met if $\varrho(k) > 0$, i.e., $k = k_i$, the control input is:

$$\begin{aligned} u(k) &= u(k-1) + \\ &+ \frac{\hat{\varphi}(k)}{(\hat{\varphi}^2(k) + \tau)(1 + mT)}\lambda(k) \\ &+ \frac{(\hat{\varphi}^2(k) + 2\tau)\,\hat{\varphi}(k)q(k)}{(\hat{\varphi}^2(k) + \tau)^2} \end{aligned} \tag{19}$$

Where $q(k) = y_d(k+1) - \hat{y}_a(k) - (2 + k_a)\,\varepsilon_a(k) + \varepsilon_a(k-1) - \frac{\varepsilon(k)}{1+mT}$.

And when $k \in [k_{i-1}, k_i)$, no sampling data is transferred and no new computations are generated, there is:

$$u(k) = u(k_{i-1}) \tag{20}$$

The block diagram of EMFASPC is shown in Fig. 1. It can be seen there are three modules, namely the event-triggered control module, observer-based PPD estimation module, and sliding mode predictive control module. The sampled data first enters the event trigger control module, where the

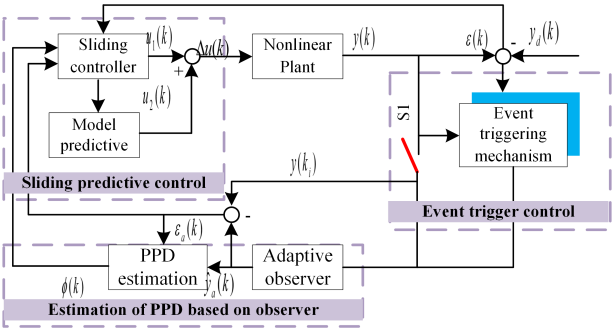

Fig. 1. Block diagram of the proposed control scheme.

triggering mechanism determines whether the triggering condition is satisfied. If it is, S1 is closed, $\beta(k) = 1$, and the data enters the sliding mode predictive control module via the PPD estimation module to generate a new control input; however, if the triggering condition is not, S1 is opened, $\beta(k) = 0$, and the PPD and the control input remain unchanged.

3.3. Stability analysis

Theorem 1. For the nonlinear system Eq. (1) satisfying Assumptions 1-2, with the controller EMFASPC(Eq. (16)), the observer-based PPD estimation algorithm Eq. (8) and the event trigger condition Eq. (17), the tracking of the desired trajectory can be achieved and the tracking error are uniformly ultimately bounded.

Proof. The stability of the system is closely related to $\hat{\varphi}(k), \varepsilon_a(k)$, and $\varepsilon(k)$. The boundedness of these parameters is discussed respectively.

1. Boundedness of $\hat{\varphi}(k)$ When $k = k_i$, the estimation algorithm is executed to calculate the PPD, $\hat{\varphi}(k) = \hat{\varphi}(k_i)$. Based on (6), subtracting its left and right sides by $\varphi(k+1)$, considering the slow time-varying property of PPD, and combining (5), we can get:

$$\breve{\varphi}(k_{i+1}) = \breve{\varphi}(k)\left(1 - 2\Delta u^2(k)\left(|\Delta u(k)|^2 + \chi\right)^{-1}\right) \tag{21}$$

Where $\chi > 0$ with $\Delta u^2(k)\left(|\Delta u(k)|^2 + \chi\right)^{-1} \in (0,1)$, and let there exist $0 < \bar{c} < 1$, such that:

$$0 < \left|1 - 2\Delta u^2(k)\left(|\Delta u(k)|^2 + \chi\right)^{-1}\right| \leq \bar{c} < 1 \tag{22}$$

Substituting into Eq. (7), while taking absolute values on both sides of the equation, we get

$$|\breve{\varphi}(k+1)| \leqslant \bar{c}|\breve{\varphi}(k)| \leqslant \cdots \leqslant \bar{c}^k|\breve{\varphi}(1)| \tag{23}$$

It can be seen that $\breve{\varphi}(k)$ is bounded, so $\hat{\varphi}(k_i)$ is bounded.

When $k \in [k_i - 1, k_i)$, it belongs to the region where the trigger condition is not satisfied, $\hat{\varphi}(k) = \hat{\varphi}(k_{i-1})$, just discussed that $\hat{\varphi}(k_i)$ is bounded, so the non-trigger instant $\hat{\varphi}(k)$ is also bounded.

2. Boundedness of $\varepsilon_a(k)$

Define the Lyapunov function $V_\varepsilon(k) = \frac{1}{2}\theta\varepsilon_a(k)^2, \theta > 0$, and substitute Eqs. (4) and (5):

$$\begin{aligned}
&\Delta V_\varepsilon(k+1) = \frac{1}{2}\theta\left(K_a^2 - 2K_a\right)\varepsilon_a^2(k) + \\
&\theta\left(1 - K_a\right)\varepsilon_a(k)\Delta u(k)\breve{\varphi}(k) + \frac{1}{2}\theta\Delta u^2(k)\breve{\varphi}^2(k) \\
&\leq \frac{\theta}{2}\left(K_a^2 - 2K_a + \frac{1}{2}\varepsilon\theta^2\right)\varepsilon_a^2(k) + \\
&\left(\frac{1}{2}\theta + \frac{1}{2\varepsilon}\left(1 - K_a\right)^2\right)\Delta u^2(k)\breve{\varphi}^2(k)
\end{aligned} \tag{24}$$

Since $0 < K_a < 1$, there is $K_a^2 - 2K_a < 0$. If the polynomial $\frac{\theta}{2}\left(K_a^2 - 2K_a + \frac{1}{2}\varepsilon\theta^2\right)$ and $\frac{1}{2}\theta + \frac{1}{2\varepsilon}(1 - K_a)^2$ are less than 0 , then $\Delta V_\varepsilon(k) < 0$. In this way, $\Delta V_\varepsilon(k) \to 0$ when $k \to \infty, \varepsilon_a(k)$ is bounded and $\lim_{k\to\infty}\varepsilon_a(k) = 0$

3. Boundedness of $\varepsilon(k)$ In the operation of the controller, the sliding surface function plays a crucial role, so we discuss the boundedness of the sliding surface before analyzing the boundedness of $\varepsilon(k)$.

Choose the Lyapunov function $V_\lambda(k) = \lambda(k)^2$, one can obtain:

$$\begin{aligned}
&\Delta V_\lambda(k+1) = \left(-\frac{\hat{\varphi}^2(k)}{\hat{\varphi}^2(k)+\tau}\lambda(k) + \frac{\tau^2(1+mT)}{\left(\hat{\varphi}^2(k)+\tau\right)^2}q(k)\right. \\
&\left. + 2\lambda(k)\right)\left(\frac{\tau^2(1+mT)}{\left(\hat{\varphi}^2(k)+\tau\right)^2}q(k) - \frac{\hat{\varphi}^2(k)}{\mathfrak{S}^2(k)+\tau}\lambda(k)\right) \\
&= -\frac{\hat{\varphi}^2(k)\left(\hat{\varphi}^2(k)+2\tau\right)}{\left(\hat{\varphi}^2(k)+\tau\right)^2}\lambda(k)^2 + j_1(k)\lambda(k) + j_2(k)
\end{aligned} \tag{25}$$

where $j_1(k) = \frac{2\tau^3(1+mT)}{\left(\hat{\varphi}^2(k)+\tau\right)^3}q(k)$ and $j_2(k) = \frac{\tau^4(1+mT)^2}{\left(\hat{\varphi}^2(k)+\tau\right)^4}q^2(k)$, since $\tau > 0$, there must be $\frac{\hat{\varphi}^2(k)\left(\hat{\varphi}^2(k)+2\tau\right)}{\left(\hat{\varphi}^2(k)+\tau\right)^2} > 0$

that is, the coefficient of $\lambda^2(k)$ is less than 0 . Let $j_0(k) \leq \frac{\hat{\varphi}^2(k)\left(\hat{\varphi}^2(k)+2\tau\right)}{\left(\hat{\varphi}^2(k)+\tau\right)^2}$, substituting Eq. (34) we have:

$$\Delta V_\lambda(k+1) \leq -j_0(k)\lambda^2(k) + j_1(k)\lambda(k) + j_2(k) \tag{26}$$

so when $\lambda(k) > \left(j_1(k) + \sqrt{j_1^2(k) + 4j_0(k)j_2(k)}\right) / \left(2j_0(k)\right)$, $\Delta V(k+1) < 0$, $\lambda(k)$ is bounded and there exists $\lim_{k\to\infty}|\lambda(k)| \leq \left(j_1(k) + \sqrt{j_1^2(k) + 4j_0(k)j_1(k)}\right) / \left(2j_0\right) = M$, where M is for the convenience of subsequent use.

When $k = k_i$, one can get:

$$\begin{aligned}
&\varepsilon\left(k_i+1\right) = y_d(k+1) - \hat{y}_a(k) + \varepsilon_a(k-1) - \\
&\left(2+K_a\right)\varepsilon_a(k) - \hat{\varphi}(k)\left(\frac{\hat{\varphi}(k)\lambda(k)}{\left(\hat{\varphi}^2(k)+\tau\right)(1+mT)}\right. \\
&\left. + \frac{\left(\hat{\varphi}^2(k)+2\tau\right)\hat{\varphi}(k)q(k)}{\left(\hat{\varphi}^2(k)+\tau\right)^2}\right) \\
&= \frac{\tau^2}{\left(\hat{\varphi}^2(k)+\tau\right)^2}\Pi(k) + \frac{\hat{\varphi}^2(k)\left(\hat{\varphi}^2(k)+2\tau\right)\varepsilon\left(k_i\right)}{\left(\hat{\varphi}^2(k)+\tau\right)^2(1+mT)} \\
&- \frac{\hat{\varphi}^2(k)\lambda(k)}{\left(\hat{\varphi}^2(k)+\tau\right)(1+mT)}
\end{aligned} \tag{27}$$

where $\hat{\varphi}(k) = \hat{\varphi}\left(k_i\right)$, $\Pi(k) = y_d(k+1) - \hat{y}_a(k) - \left(2+K_a\right)\varepsilon_a(k) + \varepsilon_a(k-1)$ at the trigger instant can also be transformed after further simplification:

$$\begin{aligned}
\Pi(k) =& y_d(k+1) - o(k) - y\left(k_i\right) - \\
&\left(1+K_a\right)\varepsilon_a(k) + \varepsilon_a(k-1) \\
=& \Delta y_d(k+1) + \varepsilon\left(k_i\right) - \\
&\left(1+K_a\right)\varepsilon_a(k) + \varepsilon_a(k-1)
\end{aligned} \tag{28}$$

Let $\frac{mT}{1+mT} = d_1$, because $0 < mT < 1 + mT$, so $0 < d_1 < 1$. Let $\frac{\hat{\varphi}^2(k)\left(\hat{\varphi}^2(k)+2\tau\right)}{\left(\hat{\varphi}^2(k)+\tau\right)^2} = d_2$, and $\tau > 0$ determines that $0 < \hat{\varphi}^2(k)\left(\hat{\varphi}^2(k)+2\tau\right) < \left(\hat{\varphi}^2(k)+\tau\right)^2$, so $0 < d_2 < 1$, thereby, $0 < 1 - d_1 d_2 = d_3 < 1$. If the symbols H_1 and H_2 are used to denote $\frac{\tau^2}{\left(\hat{\varphi}^2(k)+\tau\right)^2}$ and $\frac{\hat{\varphi}^2(k)\lambda(k)}{\left(\hat{\varphi}^2(k)+\tau\right)(1+mT)}$, combined with Eqs. (27) and (28):

$$\begin{aligned}
&\left|\varepsilon\left(k_i+1\right)\right| \leq d_3\left|\varepsilon\left(k_i\right)\right| + 2H_1A + H_2|\lambda(k)| \\
&\leq d_3^2\left|\varepsilon\left(k_i-1\right)\right| + d_3\left(2H_1A + H_2|\lambda(k)|\right) + \\
&2H_1A + H_2|\lambda(k)| \leq \cdots \\
&\leq d_3^k|\varepsilon(1)| + \frac{\left(2H_1A + H_2|\lambda(k)|\right)\left(1 - d_3^k\right)}{1 - d_3}
\end{aligned} \tag{29}$$

Substituting boundary M, one can get:

$$\lim_{k\to\infty}\left|\varepsilon\left(k_i\right)\right| \leq \frac{2H_1A + H_2M}{1 - d_3} \tag{30}$$

where $k \in [k_i, k_{i+1})$, there are no estimates of the PPD and update of input, which is equivalent to $\Delta u(k) = 0$, and the tracking error at this time:

$$\begin{aligned}|\varepsilon(k+1)| =&|\Pi(k)-\Delta u(k)\hat{\varphi}(k)|\\ =&|\Delta y_d(k+1)-o(k)+\varepsilon(k_i)\\ &+\varepsilon_a(k-1)-(1+K_a)\varepsilon_a(k)|\\ \leq&|\vartheta||\varepsilon(k)|+|\varepsilon(k_i)|+2A\end{aligned} \tag{31}$$

Since $0<\vartheta<1$, it follows that:

$$\lim_{k\to\infty}|\varepsilon(k)|\leq\frac{H_2M+2A(H_1+1-d_3)}{(1-d_3)(1-\vartheta)} \tag{32}$$

Moreover, if $\sigma\to 0, A\to 0, m\to\infty$, the tracking error satisfies $\lim_{k\to\infty}|\varepsilon(k)|\to 0$ whether it is triggered instantaneously or not, i.e., the control system is asymptotically stable.

4. Simulation

In this section, we confirm the effectiveness of the proposed method through two simulation experiments. The first one is a numerical simulation and the second one is a simulation of an industrial shell and tube heat exchanger control system. The design of the controller does not depend on the given mathematical model but on the input and output data generated by the system.

4.1. Example 1

The SISO nonlinear system is selected as follows:

$$\begin{aligned}y(k+1)=&a(k)\frac{y(k)+0.1}{1+y(k)^2}+\\ &b(k)(y(k)+1)u(k)+c(k)u(k)^3\end{aligned} \tag{33}$$

where a(k)=1+0.2 sin $\frac{2k\pi}{400}$, $b(k)=0.5+\frac{0.2k}{400}$ and $c(k)=\exp\left(\frac{-k}{400}\right)$.

The desired tracking trajectory is as follows:

$$\begin{aligned}y_d(k+1)=&0.5+0.2(\sin((1.3k\pi/100)+\\ &\sin((1.5k\pi/170))+\sin((k\pi/200)))\end{aligned} \tag{34}$$

Set the parameters for the proposed EMFASPC as $K_a=0.85,\sigma=75,\vartheta=0.8,\lambda=1.8,\delta=10^{-5}$, $m=1.75,\hat{\psi}(1)=2,\tau=0.02,v=0.01$. The static event-driven proportional sliding mode model-free adaptive control (et-MFAC) proposed in [22] is compared with the proposed controller to demonstrate the superiority of EMFASPC in terms of control accuracy. Its parameters are $\hat{\psi}(1)=4.3$, $K_o=0.05,\mu=1.8,\varepsilon=0.001,\lambda=100,\sigma=1e-4,\beta=0.9,\omega=0.5,\xi=0.0035$, and $K_f=0.5$.

As can be seen from Fig. 2(a), which displays their output characteristics, the proposed method has superior tracking accuracy and can finish the tracking work more quickly. Although both controllers use the event-triggered to perform the tracking of the desired trajectory, the proposed controller has a better tracking performance due to the introduction of predictive control and the modification of the event-triggered mechanism (see Fig. 2(b) & (c)) is the PPD estimation curve, and the proposed algorithm has a smaller overshoot and less variation, which is conducive to the fast stabilization of the system. Fig. 2(d) indicates the instant at which each trigger event occurs. Further, the number of triggers for EMFASPC and et-MFAC are 477 and 624, respectively, within [0,1000] moments, which saves 14.7% of the network bandwidth while achieving superior tracking results. Fig. 2(e) and Fig. 2(f) depict the interval times between adjacent events for both algorithms. It can be seen that the proposed interval time is short and more evenly distributed, the interval time of et-MFAC is uneven, and when a long interval time event occurs, it has to be compensated by many short interval events, requiring multiple updates of the control input for compensation, wasting transmission bandwidth and making tracking less effective than the former.

Also, in the suggested controller, the system's output performance is impacted by the v option. The output curves for $v=0.01, v=1$, and $v=100$ are displayed in Fig. 3(a). while $\vartheta=0.8$ remains constant. As can be seen, when v rises, the output overshoot decreases while the tracking precision deteriorates. The number of events events triggered at three different v are shown in Fig. 3(b) if ϑ is changed and the values $[0.1,0.2,0.3,0.4,0.5,0.6,0.7,0.8,0.9,1]$ are chosen, respectively. It is clear that as ϑ increases from 0.1 to 1 , the number of events triggered at various v decreases in terms of the number of triggers. Consequently, it is important to choose the value of v sensibly when balancing tracking speed, tracking precision, and bandwidth consumption.

4.2. Example 2

Heat exchangers are commonly used in industrial production temperature control devices, they can be divided into three main categories according to the principle of cold and hot fluid heat exchange, namely: inter-wall, hybrid, and thermal storage types. Among them, the inter-wall heat exchanger is the most used. The shell and tube heat exchanger is the most widely used between the wall heat exchanger. However, it has confident uncertain nonlinear behavior limited by operating conditions and material properties.

While the shell-and-tube heat exchanger is in use, cold fluid enters from the liquid intake, travels through the tube bundle, and then exits from the liquid outlet, as shown in Fig. 4. The steam intake allows hot liquid to enter, which flows around the heat exchanger's tube sheet and tube

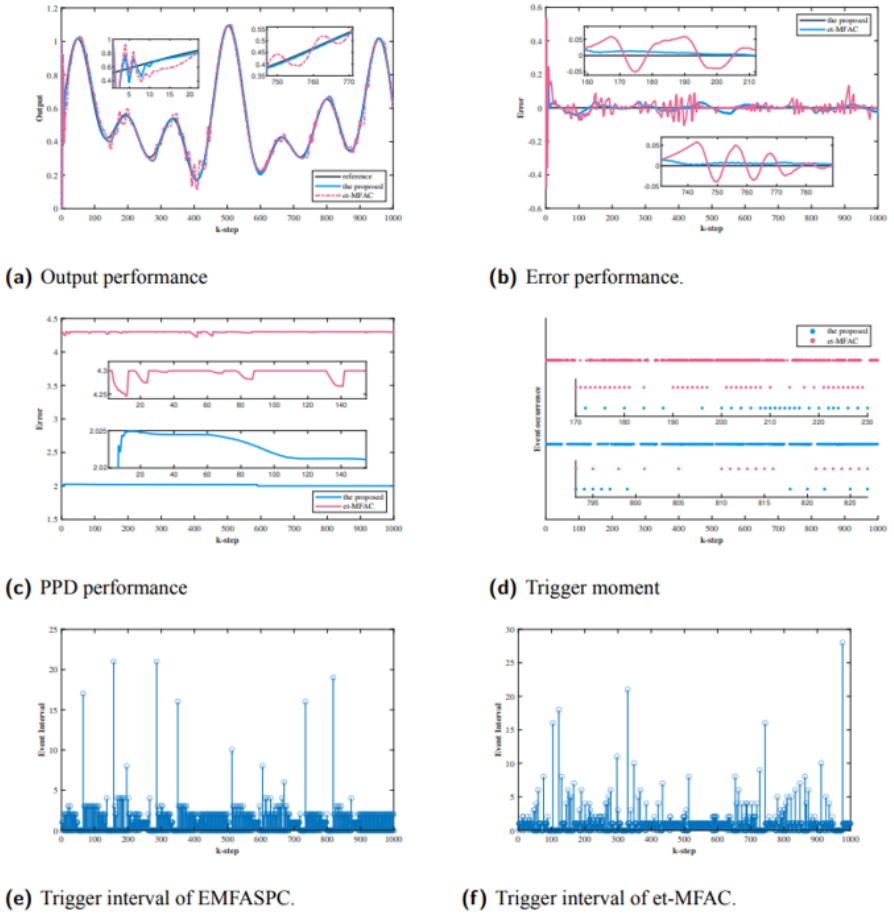

(a) Output performance **(b)** Error performance.

(c) PPD performance **(d)** Trigger moment

(e) Trigger interval of EMFASPC. **(f)** Trigger interval of et-MFAC.

Fig. 2. Tracking performance under different schemes.

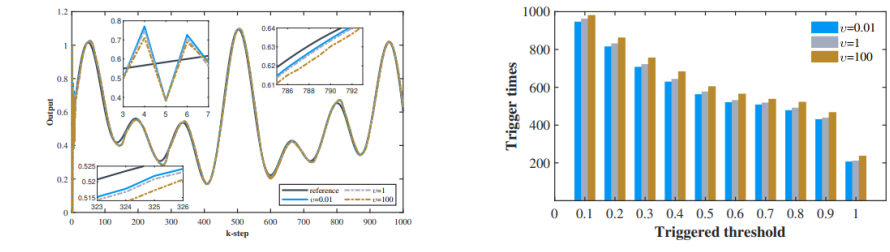

(a) Different υ. **(b)** Different υ and ϑ.

Fig. 3. Output performance and number of triggers under ν

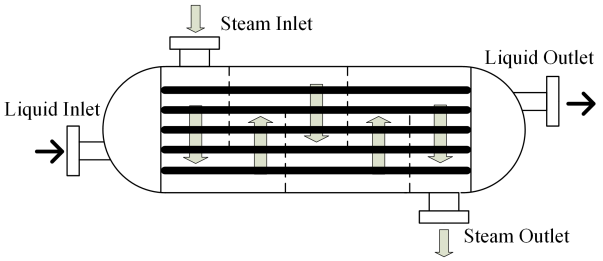

Fig. 4. Internal structure of shell and tube heat exchanger.

bundle and out the steam outlet. A number of the tube bundle's thin tube walls serve as a barrier between the hot fluid and the cold fluid. To complete the entire heat transfer process, the hot fluid first transfers heat to the thin tube wall, which then does the same for the cold fluid inside the tube.

In this paper, the dynamic behavior of the heat exchanger is described by the Hammerstein model of [30] with the process water flow as the input and the process water outlet temperature as the output under the condition of keeping the steam flow constant:

$$\begin{aligned} G_H\left(z^{-1}\right) &= \frac{1.2z^{-1}-0.1z^{-2}}{1-0.6z^{-1}+0.1z^{-2}} \\ N(u) &= 1.5u(k) - 1.5u^2(k) + 0.5u^3(k) \end{aligned} \tag{35}$$

Set the following parameters for the proposed controller: $\tau = 0.02, \sigma = 60, \vartheta = 0.3, \hat{\psi}(1) = 2.5, \lambda = 1.6$ and the rest of the parameters are the same as above. The parameter $\xi = 0.0015$ for the et-MFAC [22] is used for comparison, and the rest of the parameters also remain the same. The simulation results of the two control algorithms are shown in Figs. 5 and 6, where Fig. 5(a) and Fig. 5(b) show the output and tracking error performance of the system. At operating points 0, 300, 500, and 750, where the desired value varies widely and the proposed controller can respond quickly to adjust the output with less tracking error, while when the desired value is constant, the EMFASPC has higher control accuracy than the et-MFAC due to the predictive control optimized control input. EMFASPC and et-MFAC use the event-driven approach rather than continuously updating their respective control inputs.

Their event triggers in 10,00 operational points are 329 and 494 , respectively, demonstrating that the proposed strategy is more favorable in terms of computational resource savings. When the operating point has a constant desired value, as illustrated in Fig. 6(a) and Fig. 6(b), it can be shown that the suggested approach will remain untriggered for a longer duration with fewer triggers, freeing up more valuable bandwidth while ensuring a smaller tracking error.

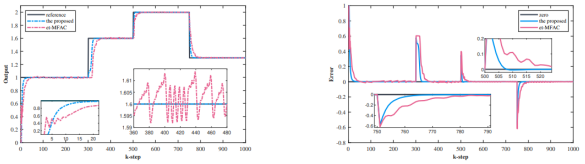

(a) Output of heat exchanger. **(b)** Error of heat exchanger.

Fig. 5. Tracking performance of shell and tube heat exchanger.

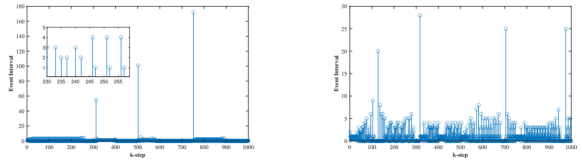

(a) Trigger interval under EMFASPC **(b)** Trigger interval under et-MFAC

Fig. 6. Trigger performance of shell and tube heat exchanger.

5. Conclusion

In this paper, we propose an EMFASPC scheme for the trajectory tracking problem of discrete-time nonlinear systems from the perspective of saving network bandwidth and computational resources. It is a combination of MFAC, SMC, and MPC, uses a CFDL method to create the PPD data model based on adaptive observers, and achieves rolling optimization in the predicted time domain based on the prediction of discrete integral sliding mode surface functions. At each moment, the relationship of trigger error, event trigger threshold, and tracking error is used to decide whether the PPD and control input are updated or maintained, which realizes the conversion from periodic update to the acyclic transmission of traditional data and reduces the burden of signal transmission. The advantages of the proposed algorithm in terms of control accuracy and bandwidth utilization are verified through numerical simulations and shell-and-tube heat exchanger system simulations. In the next step, we will consider model-free adaptive control in a non-periodic manner for multi-input and multi-output systems.

Acknowledgment

This work was funded by National Natural Science Foundation of China (51967012), Key Research and Development Program of Gansu Province (20YF8GA055), Natural Science Foundation of Gansu Province (22JR5RA359,22JR5RA353).

References

[1] Z. Hou. *Model Free Adaptive Control: Theory and Applications*. Model Free Adaptive Control: Theory and Applications, 2013. DOI: 10.1201/b15752.

[2] Z. Hou and S. Jin, (2010) *"A novel data-driven control approach for a class of discrete-time nonlinear systems"* **IEEE Transactions on Control Systems Technology** ***19***(6): 1549–1558. DOI: 10.1109/TCST.2010.2093136.

[3] S. Xiong and Z. Hou, (2020) *"Model-free adaptive control for unknown MIMO nonaffine nonlinear discrete-time systems with experimental validation"* **IEEE Transactions on Neural Networks and Learning Systems** ***33***(4): 1727–1739. DOI: 10.1109/TNNLS.2020.3043711.

[4] D. Xu, B. Jiang, and P. Shi, (2013) *"Adaptive observer based data-driven control for nonlinear discrete-time processes"* **IEEE transactions on automation science and engineering** ***11***(4): 1037–1045. DOI: 10.1109/TASE.2013.2284062.

[5] D. Xu, Y. Shi, and Z. Ji, (2017) *"Model-free adaptive discrete-time integral sliding-mode-constrained-control for autonomous 4WMV parking systems"* **IEEE Transactions on Industrial Electronics** ***65***(1): 834–843. DOI: 10.1109/TIE.2017.2739680.

[6] M. Hou and Y. Wang, (2021) *"Data-driven adaptive terminal sliding mode control with prescribed performance"* **Asian Journal of Control** ***23***(2): 774–785. DOI: 10.1002/asjc.2245.

[7] Y. Zhao, X. Liu, H. Yu, and J. Yu, (2020) *"Model-free adaptive discrete-time integral terminal sliding mode control for PMSM drive system with disturbance observer"* **IET Electric Power Applications** ***14***(10): 1756–1765. DOI: 10.1049/iet-epa.2019.0966.

[8] Y. Weng and X. Gao, (2016) *"Data-driven robust output tracking control for gas collector pressure system of coke ovens"* **IEEE Transactions on Industrial Electronics** ***64***(5): 4187–4198. DOI: 10.1109/TIE.2016.2613509.

[9] X. Shi, Y. Cao, Y. Li, J. Ma, M. Shahidehpour, X. Wu, and Z. Li, (2020) *"Data-driven model-free adaptive damping control with unknown control direction for wind farms"* **International Journal of Electrical Power & Energy Systems** ***123***: 106213. DOI: 10.1016/j.ijepes.2020.106213.

[10] S. Li, D. Sauter, and B. Xu, (2015) *"Co-design of event-triggered H∞ control for discrete-time linear parameter-varying systems with network-induced delays"* **Journal of the Franklin Institute** ***352***(5): 1867–1892. DOI: 10.1016/j.jfranklin.2015.02.001.

[11] M. Abdelrahim, R. Postoyan, and J. Daafouz, (2015) *"Event-triggered control of nonlinear singularly perturbed systems based only on the slow dynamics"* **Automatica** ***52***: 15–22. DOI: 10.1016/j.automatica.2014.10.125.

[12] L. Zou, Z. Wang, H. Gao, and X. Liu, (2015) *"Event-triggered state estimation for complex networks with mixed time delays via sampled data information: The continuous-time case"* **IEEE Transactions on Cybernetics** ***45***(12): 2804–2815. DOI: 10.1109/TCYB.2014.2386781.

[13] A. Sahoo, X. Hao, and S. Jagannathan, (2016) *"Near Optimal Event-Triggered Control of Nonlinear Discrete-Time Systems Using Neurodynamic Programming"* **IEEE Transactions on Neural Networks & Learning Systems** ***27***(9): 1801–1815. DOI: 10.1109/TNNLS.2015.2453320.

[14] W. Heemels and M. Donkers, (2013) *"Periodic event-triggered control for linear systems"* **IEEE Transactions on Automatic Control** ***49***(3): 698–711. DOI: 10.1016/j.ijepes.2023.109278.

[15] L. Ma, Z. Wang, H.-K. Lam, and N. Kyriakoulis, (2016) *"Distributed event-based set-membership filtering for a class of nonlinear systems with sensor saturations over sensor networks"* **IEEE transactions on cybernetics** ***47***(11): 3772–3783. DOI: 10.1109/TCYB.2016.2582081.

[16] L. Ding, Q. L. Han, X. Ge, and X. M. Zhang, (2018) *"An Overview of Recent Advances in Event-Triggered Consensus of Multiagent Systems"* **IEEE Transactions on Cybernetics** ***48***(4): 1110–1123. DOI: 10.1109/TCYB.2017.2771560.

[17] D. Liu and G. H. Yang, (2017) *"Event-Based Model-Free Adaptive Control for Discrete-Time Nonlinear Processes"* **Iet Control Theory & Applications** ***11***(15): 2531–2538.

[18] D. Liu and G.-H. Yang, (2018) *"Neural network-based event-triggered MFAC for nonlinear discrete-time processes"* **Neurocomputing** ***272***: 356–364. DOI: 10.1016/j.neucom.2017.07.008.

[19] N. Lin, R. Chi, and B. Huang, (2019) *"Event-triggered model-free adaptive control"* **IEEE Transactions on Systems, Man, and Cybernetics: Systems** ***51***(6): 3358–3369. DOI: 10.1109/TSMC.2019.2924356.

[20] Y. Wang, X. Qiu, H. Zhang, and X. Xie, (2021) *"Data-driven-based event-triggered control for nonlinear CPSs against jamming attacks"* **IEEE Transactions on Neural Networks and Learning Systems** ***33***(7): 3171–3177. DOI: 10.1109/TNNLS.2020.3047931.

[21] H. F. Li, Y. C. Wang, and H. G. Zhang, (2019) *"Data-driven-based event-triggered tracking control for nonlinear systems with unknown disturbance"* **Control Theory & Applications, IET *13***(14): 2197–2206. DOI: 10.1049/iet-cta.2019.0051.

[22] C. Gao, W. Zhang, D. Xu, W. Yang, and T. Pan, (2022) *"Event-triggered based model-free adaptive sliding mode constrained control for nonlinear discrete-time systems"* **International Journal of Innovative Computing, Information and Control *18***(2): 525–536. DOI: 10.24507/ijicic.18.02.525.

[23] Y. S. Ma, W. W. Che, and C. Deng, (2022) *"Event-triggered model-free adaptive control for nonlinear cyber-physical systems with false data injection attacks"* **International Journal of Robust and Nonlinear Control *32***(4): 2442–2452. DOI: 10.1002/rnc.5958.

[24] J. Liu, Member, IEEE, S. Vazquez, and S. Member, (2016) *"Extended State Observer-Based Sliding-Mode Control for Three-Phase Power Converters"* **IEEE Transactions on Industrial Electronics *64***(1): 22–31. DOI: 10.1109/TIE.2016.2610400.

[25] W. Garcia-Gabin, D. Zambrano, and E. F. Camacho, (2009) *"Sliding mode predictive control of a solar air conditioning plant"* **Control Engineering Practice *17***(6): 652–663. DOI: 10.1016/j.conengprac.2008.10.015.

[26] Q. Xu, (2016) *"Digital Integral Terminal Sliding Mode Predictive Control of Piezoelectric-Driven Motion System"* **IEEE Transactions on Industrial Electronics *63***(6): 3976–3984. DOI: 10.1109/TIE.2015.2504343.

[27] S. Kang, H. Wu, X. Yang, Y. Li, J. Yao, B. Chen, and H. Lu, (2021) *"Discrete-time predictive sliding mode control for a constrained parallel micropositioning piezostage"* **IEEE Transactions on Systems, Man, and Cybernetics: Systems *52***(5): 3025–3036. DOI: 10.1109/TSMC.2021.3062581.

[28] H. Li, H. Yang, F. Sun, and Y. Xia, (2014) *"Sliding-Mode Predictive Control of Networked Control Systems Under a Multiple-Packet Transmission Policy"* **IEEE Transactions on Industrial Electronics *61***(11): 6234–6243. DOI: 10.1109/TIE.2014.2311411.

[29] Z. Tian, J. Yuan, X. Zhang, L. Kong, and J. Wang, (2018) *"Modeling and sliding mode predictive control of the ultra-supercritical boiler-turbine system with uncertainties and input constraints"* **ISA transactions *76***: 43–56. DOI: 10.1016/j.isatra.2018.03.004.

[30] E. Eskinat, S. H. Johnson, and W. L. Luyben, (1991) *"Use of Hammerstein models in identification of nonlinear systems"* **AIChE Journal *37***(2): 255–268. DOI: 10.1002/aic.690370211.